the other AD-water molecule to form an AAD-water molecule with the acceptance of one more proton. As schematically shown in Fig. 3C, when all of the water molecules are three-coordinated (AAD and ADD), the hydrogen bond network should have a 3D cage structure in which each water molecule is located at the vertex of the polyhedral cages, because of the tetrahedral coordination nature of the water hydrogen bond. On the basis of mass spectrometry and ab initio calculations, the structure of cluster $n = 21$ has been suggested to be a regular dodecahedron cage that includes one water inside the cage (*1*, *2*, *9*, *10*). Many nearly isoenergetic structural isomers, including the 2D net types, may contribute to the present IR spectra because of the internal energy of the clusters. However, the dominance of the AAD dangling OH band intensity over the AD dangling OH band intensity in $n \geq 21$ clearly indicates that the 2D net types are converted to 3D cage structures in this size region. Such nanometer-sized cage structures have not previously been experimentally confirmed for hydrogen-bonded cluster systems. The central H_3O^+ or $H_2O_5^+$ ion core prefers the planar coordination by nature, and it allows 3D cage formation only in such large-sized clusters.

References and Notes

1. U. Nagashima, N. Nishi, H. Tanaka, *J. Chem. Phys.* **84**, 209 (1986).
2. S. Wei, Z. Shi, A. W. Castleman Jr., *J. Chem. Phys.* **94**, 3268 (1991).
3. T. F. Magnera, D. E. David, J. Michl, *Chem. Phys. Lett.* **182**, 363 (1991).
4. N. F. Dalleska, K. Honma, P. B. Armentrout, *J. Am. Chem. Soc.* **115**, 12125 (1993).
5. L. I. Yeh, M. Okumura, J. D. Myers, J. M. Price, Y. T. Lee, *J. Chem. Phys.* **91**, 7319 (1989).
6. M. Okumura, L. I. Yeh, J. D. Myers, Y. T. Lee, *J. Phys. Chem.* **94**, 3416 (1990).
7. J.-C. Jiang *et al.*, *J. Am. Chem. Soc.* **122**, 1398 (2000).
8. S. J. Singer, S. McDonald, L. Ojamäe, *J. Chem. Phys.* **112**, 710 (2000).
9. A. Khan, *Chem. Phys. Lett.* **319**, 440 (2000).
10. M. P. Hodges, D. J. Wales, *Chem. Phys. Lett.* **324**, 279 (2000).
11. F. Huisken, M. Kaloudis, A. Kulcke, *J. Chem. Phys.* **104**, 17 (1996).
12. K. Liu *et al.*, *Nature* **381**, 501 (1996).
13. R. N. Pribble, T. S. Zwier, *Science* **265**, 75 (1994).
14. M. Miyazaki, A. Fujii, T. Ebata, N. Mikami, *Phys. Chem. Chem. Phys.* **5**, 1137 (2003).
15. Protonated water clusters were produced by a photo-assisted discharge of water vapor seeded in Ne (total pressure 3 atm). The gas mixture was expanded from a pulsed supersonic valve through a channel nozzle (*23*). The channel was equipped with a wire electrode at its sidewall, and a dc voltage of −300 V relative to the channel was applied to the electrode. The discharge in the channel was triggered by irradiation of the electrode surfaces with a laser pulse (355 nm, ~5 mJ/pulse), which was synchronized with the pulsed valve operation. The protonated water cluster cations were cooled on expansion from the channel. The size distribution of the produced cluster cations was similar to those reported so far (*1*), and the magic number at $n = 21$ was also seen.
16. We observed that 3 to 10% of the parent-cluster cations spontaneously dissociate after passing through the first quadrupole mass filter. Evaporation of one water molecule was the unique dissociation pass.
17. V. Buch, J. P. Devlin, *J. Chem. Phys.* **94**, 4091 (1991).
18. J. C. Jiang *et al.*, *Chem. Phys. Lett.* **289**, 373 (1998).
19. B. Rowland, M. Fisher, J. P. Devlin, *J. Chem. Phys.* **95**, 1378 (1991).
20. C. J. Gruenloh *et al.*, *Science* **276**, 1678 (1997).
21. U. Buck, I. Ettischer, M. Melzer, V. Buch, J. Sadlej, *Phys. Rev. Lett.* **80**, 2578 (1998).
22. J. P. Devlin, J. Sadlej, V. Buch, *J. Phys. Chem. A* **105**, 974 (2001).
23. S. Sato, T. Ebata, N. Mikami, *Spectrochim. Acta* **50A**, 1413 (1994).

24. We are grateful to H. Ishikawa and T. Maeyama for useful discussions and to H. Kawamata for his contribution to the IR laser system construction.

26 January 2004; accepted 19 March 2004
Published online 29 April 2004;
10.1126/science.1096037
Include this information when citing this paper.

Infrared Signature of Structures Associated with the $H^+(H_2O)_n$ ($n = 6$ to 27) Clusters

J.-W. Shin,[1] N. I. Hammer,[1] E. G. Diken,[1] M. A. Johnson,[1]* R. S. Walters,[2] T. D. Jaeger,[2] M. A. Duncan,[2]* R. A. Christie,[3] K. D. Jordan[3]*

We report the OH stretching vibrational spectra of size-selected $H^+(H_2O)_n$ clusters through the region of the pronounced "magic number" at $n = 21$ in the cluster distribution. Sharp features are observed in the spectra and assigned to excitation of the dangling OH groups throughout the size range $6 \leq n \leq 27$. A multiplet of such bands appears at small cluster sizes. This pattern simplifies to a doublet at $n = 11$, with the doublet persisting up to $n = 20$, but then collapsing to a single line in the $n = 21$ and $n = 22$ clusters and reemerging at $n = 23$. This spectral simplification provides direct evidence that, for the magic number cluster, all the dangling OH groups arise from water molecules in similar binding sites.

The nature of the proton in water is one of the most fundamental aspects of aqueous chemistry, and one important aspect of the aqueous proton is its anomalously high mobility (*1*, *2*). This phenomenon immediately introduces the crucial role of H_3O^+ and $H_5O_2^+$, the so-called Eigen (*3*) and Zundel (*4*) forms of the cation, respectively. Fluctuations between these species (*1*, *2*) are thought to mediate the Grotthuss mechanism (*5*) for proton transport, and accurate simulations of this process require quantum treatment of the hydrogen motion in the complex network environment of bulk water.

A powerful way to test the validity of various theoretical methods is through the use of the cluster ions (*6*), $H^+(H_2O)_n$, which can be prepared and isolated in the laboratory. Here, we report size-selected vibrational spectra of the $H^+(H_2O)_n$ clusters in the intermediate size regime, $6 \leq n \leq 27$, chosen to explore the putative role (*7*–*12*) of dodecahedral clathrate structures in the region around $n = 21$. The resulting spectra are analyzed with the aid of calculated structures and vibrational frequencies of selected isomers for the $n = 20$ and $n = 21$ clusters.

Protonated water clusters have been studied for decades (*3*, *4*, *7*–*18*), and in the small size regime ($n \leq 8$) vibrational spectra have been reported and interpreted with ab initio theory (*17*). H_3O^+ itself is C_{3v} pyramidal (*13*), but adding a second water molecule leads to a symmetrical sharing of the proton in the $H_2O\cdots H^+\cdots OH_2$ Zundel arrangement (*4*, *18*). Larger protonated water clusters possess multiple low-energy isomers with both Eigen and Zundel forms of the cation, and the complexity of the observed spectra indicate that several isomers are present under experimental conditions.

One of the most curious aspects of the $H^+(H_2O)_n$ clusters is Searcy and Fenn's (*7*) report in 1974 of the discontinuity in the cluster ion intensity distribution or "magic number" at $n = 21$ (Fig. 1). There has been much speculation about the structure of the magic number cluster, especially because water clathrates are known to trap methane and other gases in water cages composed of water dodecahedrons (*19*). Indeed, Searcy and Fenn (*7*) suggested that $H^+(H_2O)_{21}$ is also derived from the pentagonal dodecahedron motif, with one water molecule in the cage and the H_3O^+ ion on the surface.

In 1991, Castleman and co-workers reported a "titration" of dangling H atoms by attaching trimethylamine (TMA) molecules to the $H^+(H_2O)_{21}$ cluster (*9*). They found a drop-off in the propensity to attach the 11th TMA molecule, which suggested that 10 H atoms are free (i.e., not engaged in H-bonding) in the $H^+(H_2O)_{21}$ cluster. Because this is the same number as in the

[1]Sterling Chemistry Laboratory, Yale University, Post Office Box 208107, New Haven, CT 06520, USA. [2]Department of Chemistry, University of Georgia, Athens, GA 30602, USA. [3]Department of Chemistry, University of Pittsburgh, Pittsburgh, PA 15260, USA.

*To whom correspondence should be addressed. E-mail: mark.johnson@yale.edu (M.A.J.); maduncan@uga.edu (M.A.D.); jordan@imap.pitt.edu (K.D.J.)

neutral $(H_2O)_{20}$ dodecahedron, these authors invoked a model with the H_3O^+ species located inside the pentagonal dodecahedron, as opposed to Fenn's surface ion structure (*7*), which has only nine dangling H atoms.

Subsequent theoretical work indeed found dodecahedron-based structures to be stable. In the case of the $H^+(H_2O)_{21}$ cluster, the isomer with interior H_3O^+ was reported to be stable in Monte Carlo simulations (*10*, *16*) using model potentials. However, other model potentials (*12*, *15*) and electronic structure calculations (*11*, *14*) have indicated that the isomer with hydronium located on the surface of the cage, with a neutral H_2O molecule in the center and nine free OH groups, lies appreciably lower in energy. This discrepancy with the TMA titration results raises the possibility that the act of ligation may have driven a morphological change in the delicate balance between isomeric forms of the $H^+(H_2O)_{21}$ species.

We therefore seek a diagnostic of structure that is less disruptive than ligand titration. Vibrational spectroscopy can monitor the character of the OH stretching vibrations of the larger clusters in isolation. Recent developments in size-selected infrared (IR) spectroscopy (*20*) now enable this to be accomplished with the use of laser photodissociation: (*17*, *21*)

$$H^+(H_2O)_n + h\nu \rightarrow H^+(H_2O)_{n-1} + H_2O \quad (1)$$

Here, we report the OH stretching spectra of the protonated water clusters in the critical size range. Clusters in this size range can now be characterized theoretically by means of all-electron electronic structure methods in conjunction with flexible basis sets to evaluate whether the putative structures are consistent with these new observations.

The spectra reported here were acquired in a size-selective fashion with the use of tandem time-of-flight mass photofragmentation spectrometers (*22*, *23*). In this method, the first mass spectrometer isolates a particular cluster ion for laser excitation, and the second one selectively detects the lighter fragments that form when absorption of a photon causes water molecules to evaporate. This method recovers the actual absorption spectrum only when the cluster of interest fragments upon absorption of a photon in the excitation energy range $2000 \leq h\nu \leq 4000$ cm^{-1}. In the large cluster regime, this requirement is often at odds with the need to keep the clusters as cold as possible so that they are quenched close to their lowest-energy structures. The reported spectra were taken under strong excitation conditions (5 to 15 mJ per pulse), which typically resulted in ejection of several water molecules via sequential multiphoton absorption. Another potential complication is that the observed species may be dependent on the method of preparation. We therefore measured spectra of $H^+(H_2O)_n$ with the use of two different ion sources in different laboratories (Yale and Georgia) (*24*).

An overview of selected $H^+(H_2O)_n$ ($6 \leq n \leq 27$) spectra in the OH stretching region for clusters from the Georgia ion source is shown in Fig. 2A. As expected, the envelopes in the red-shifted range associated with H bonding (3000 to 3600 cm^{-1}) are complex and display a broad feature that blue-shifts with increasing cluster size before stabilizing into a very broad envelope stretching from 3000 to 3650 cm^{-1}. The sharpest features appear near 3700 cm^{-1}, the characteristic region of the free OH stretching vibration. Four distinct free OH band locations, labeled a to d in Fig. 2B, are observed for $H^+(H_2O)_n$. The frequencies of these bands do not vary appreciably with increasing cluster size, but rather the dominant effect is a variation of the intensity distribution among these bands.

The outer two bands (a and d) in the free OH region fall in the typical locations observed for the symmetric and asymmetric stretching vibrations of a water molecule in a single H bond–accepting configuration (i.e., where the two hydrogen atoms on the water molecule are free). As such, their presence likely reflects open structures where water molecules terminate chain-like motifs, and the disappearance of these bands for $n \geq 11$ then establishes that interconnected H-bonding networks are dominant for the larger clusters. The remaining two bands (b and c) persist throughout the size range $11 \leq n \leq 20$, with the intensity of feature c gradually being overtaken by that of feature b at $n = 12$.

An expanded view of the bands near the magic number at $n = 21$ is presented in Fig. 2C. At $n = 21$, feature c drops abruptly and is barely evident, with the $n = 22$ cluster also dominated by a single feature (b). The emergence of a single feature indicates that these sizes contain only a single class of dangling OH groups. Peak c then reappears at $n = 23$ and persists in the larger clusters studied here. The unexpected similarity of the observed vibrational spectra for $n = 21$ and $n = 22$ clusters suggests that they share a common structural motif, an observation warranting a more thorough investigation beyond the scope of the present work.

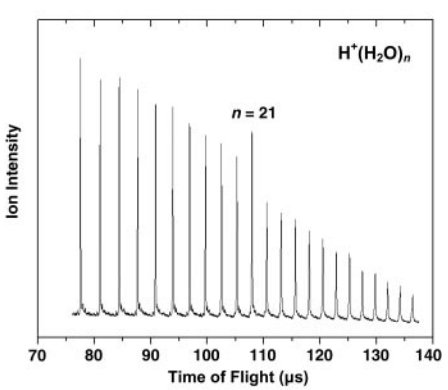

Fig. 1. Mass spectrum of $H^+(H_2O)_n$, $11 \leq n \leq 33$, obtained with the use of an electron impact ion source.

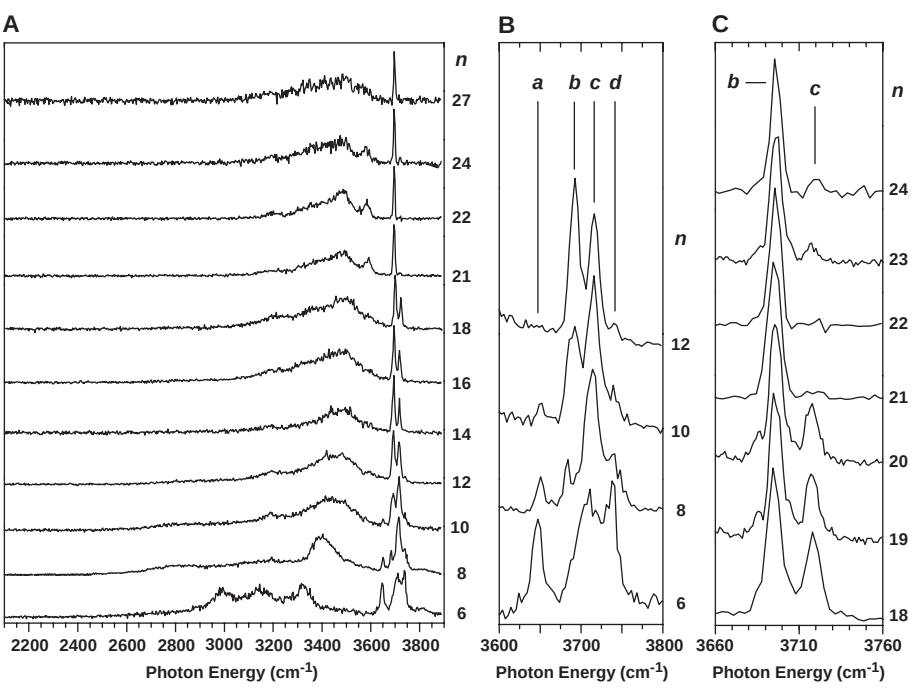

Fig. 2. Overview of the vibrational predissociation spectra of $H^+(H_2O)_n$ ($6 \leq n \leq 27$) clusters prepared with the use of the laser plasma source: (**A**) survey of the 2100 to 3900 cm^{-1} energy range, (**B**) expanded view of free OH region for smaller clusters, and (**C**) expanded view of free OH region in the critical size range around $n = 21$.

To characterize how the local binding environments affect the energies of free OH bands, we carried out electronic structure calculations (*25*, *26*) on the basis of the low energy isomers of the $n = 20$ and $n = 21$ clusters identified in earlier theoretical studies that used model potentials (*12*). For each arrangement of O atoms (*27*), we chose the isomer previously reported to be the lowest in energy (*12*). Figure 3 depicts the structures of the lowest energy (0 K) isomers (20A and 21A) recovered for the $n = 20$ and $n = 21$ clusters. Both 20A and 21A are derived from the neutral dodecahedral cluster and have an H_2O monomer inside the cage and the proton on the surface, with an Eigen-like structure (shown in blue). The structures with an interior H_3O^+ were found to lie higher in energy (~9 kcal mol^{-1} in our calculations). The present data, however, do not rule out a contribution of Castleman's high symmetry morphology to the ion ensemble (*9*). We did not recover any low-energy Zundel-based structures derived from the dodecahedron.

Isomer 20A of the $H^+(H_2O)_{20}$ cluster is calculated to have a doublet in the free OH region with a splitting similar to that found experimentally (Fig. 2C). This doublet is traced to the two types of free OH groups in 20A, those associated with AAD (A indicates acceptor and D, donor) monomers (seven in number) and that associated with a single AD water monomer (highlighted in green in Fig. 3A). The calculated spectrum for 21A, the lowest energy isomer characterized for the $n = 21$ magic number species, displays a single line in the free OH region of the spectrum as indicated in Fig. 3D, again consistent with the experimental spectrum. Interestingly, all of the free OH groups of 21A are associated with AAD monomers. Thus, our calculations offer a preliminary assignment of the observed peaks b and c (Fig. 2C) to water molecules in AAD and AD environments, respectively.

The fact that the prompt quenching of the free OH stretch doublet at $n = 21$ can be recovered in the context of the minimum energy (0 K) structures is surprising, because the cluster ensemble prepared experimentally retains substantial internal energy. In the statistical limit, for example, one can crudely estimate that the $n = 21$ cluster must contain ~1.5 eV of internal energy in order to photodissociate (on our time scale) upon excitation of a 3000 cm^{-1} photon (*28*). To qualitatively evaluate how increasing internal energy affects the spectral evolution, we obtained the spectra of $n = 20$ and $n = 21$ clusters with the use of the Yale ion source operated close to evaporative ensemble conditions (*29*), which yield the maximum internal energy constrained by evaporation kinetics. The resulting OH stretching spectra are displayed in the bottom traces in Fig. 3, C and D, for $n = 20$ and $n = 21$, respectively. Although there is a larger contribution from peak c in the spectrum from this warmer $n = 21$ cluster (Fig. 3D, bottom trace), the dramatic falloff in intensity relative to the $n = 20$ spectrum (Fig. 3C, bottom trace) is still readily apparent. Thus, the discontinuity in the OH stretching spectra in going from $n = 20$ to $n = 21$ survives even though the clusters contain substantial internal energy and therefore likely reflects the average behavior of many structurally similar isomers contributing to the ensemble. This is particularly interesting in light of the earlier observation that the "magic" intensity at $n = 21$ is an entropic phenomenon (*30*).

In the above analysis, we concentrated on the free OH bands because they provide an unambiguous diagnostic of water molecules with dangling OH groups, whereas the congested H-bonding region between 3000 and 3600 cm^{-1} is difficult to analyze in the context of structure. However, the OH stretch vibrations associated with the Eigen and Zundel ions are calculated to appear in distinct regions and should allow experimental determination of the proton environment. In particular, our calculations predict intense lines near 2500 cm^{-1} for the former and a transition below 2000 cm^{-1} for the latter. For isolated H_3O^+, the intense OH stretch vibration falls near 3500 cm^{-1} (*13*). This is redshifted to about 2800 cm^{-1} in $H^+(H_2O)_4$ (with an Eigen cation), and the band further shifts down to about 2500 cm^{-1} in the more extended H-bonded networks considered here. The calculated spectrum for structure 21A is presented in Fig. 4A, illustrating the well-isolated location of the three OH stretching transitions of the surface-embedded H_3O^+ ion. The (Georgia) experimental spectrum of the $n = 21$ cluster is displayed in Fig. 4B and is dominated by the free OH transition, and the local AAD motif assigned to this band is indicated in the inset. A relatively sharp band at around 3600 cm^{-1} emerges from the broad structure in the H-bonding region in the size range $18 \leq n \leq 24$. We can also understand this feature in the context of structure 21A, for which the calculations predict a sharp doublet in this frequency region arising from embedded DDA water molecules bound to three single-donor (AAD) water molecules.

Most puzzling, however, is that even though the calculations indicate that the observed $n = 21$ magic number and its neighbors exhibit Eigen-like structures, no photodissociation was detected below 3000 cm^{-1} for any of the larger ($n > 7$) clusters, with the relevant region indicated as H_3O^+ in Fig. 4A for $H^+(H_2O)_{21}$. Possible explanations for this include suppression of the action spectroscopy signal because of inefficient photofragmentation at the lower excitation energy of the H_3O^+ band, unexpectedly strong anharmonicity in the hydrated

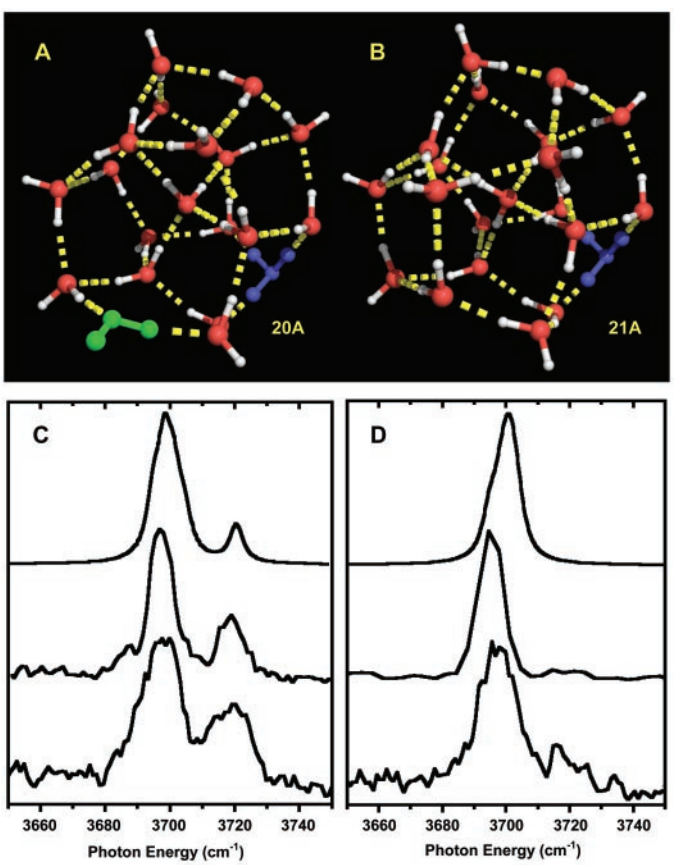

Fig. 3. Calculated lowest-energy structures of $H^+(H_2O)_n$ for $n = 20$ (**A**) and $n = 21$ (**B**). The hydronium cation is indicated in blue. For $H^+(H_2O)_{20}$ (A), the free OH responsible for the vibration absent in $H^+(H_2O)_{21}$ is indicated in green. Shown in (**C**) and (**D**) are calculated frequencies (top) and experimental spectra (middle, Georgia; bottom, Yale) of $H^+(H_2O)_n$, $n = 20$ (C) and $n = 21$ (D). The calculated spectra were obtained at the Becke3LYP/aug-cc-pVDZ† level of theory with the use of the harmonic approximation and a scale factor of 0.962. Peaks were assigned Lorentzian shapes with widths of 5 cm^{-1}.

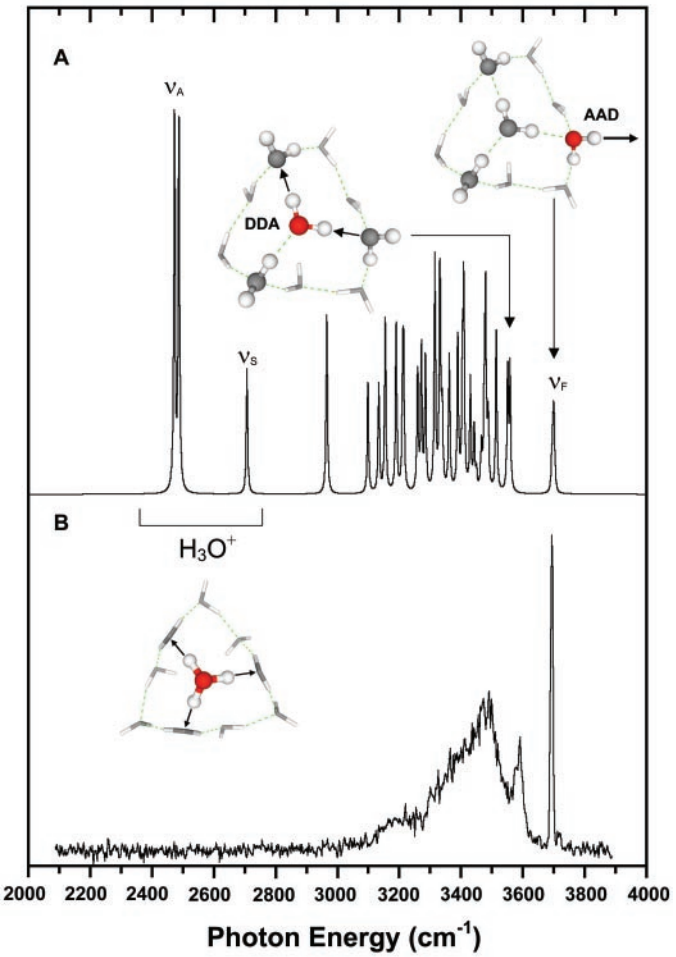

Fig. 4. Calculated [(**A**) 0.962 scaling] and experimental (**B**) vibrational predissociation spectrum of $H^+(H_2O)_{21}$. The local environments and normal mode displacements of the vibrations (discussed in the text) are depicted (arrows). AAD and DDA denote H-bond acceptor-acceptor-donor and donor-donor-acceptor motifs, and ν_A, ν_S, and ν_F refer to asymmetric, symmetric, and free OH stretches, respectively.

H_3O^+ vibrations, and finally the possibility that the proton is actually associated with a Zundel-like structure, which would "shift" the absorption due to the proton below 2000 cm^{-1}. On the basis of what is known about the smaller protonated water clusters, it seems unlikely that anharmonicity could be large enough to displace transitions associated with the H_3O^+ core below 2000 cm^{-1}. If the kinetics of photofragmentation are suppressing the lower-energy H_3O^+ band, we should be able to improve the fragmentation efficiency either by increasing the initial internal energy or by attaching a more weakly bound "messenger" atom that can be eliminated upon excitation near 2500 cm^{-1}. We therefore also scanned the low-energy region with the warmer evaporative ensemble ion source (Yale) but again failed to detect photodissociation in the critical energy range under these conditions. At the other extreme of low internal energy, a preliminary study (done at Yale, with the source tuned far from the evaporative ensemble limit discussed earlier) using an Ar messenger atom was also not successful in observing any transitions near 2500 cm^{-1} for $H^+(H_2O)_{18}$ or $H^+(H_2O)_{21}$. Thus, these IR experiments are not able to detect the predicted signature of the Eigen moiety in the larger clusters. The experiments do not rule out Zundel structures but cannot probe the crucial energy range required to establish its presence. Theory clearly favors Eigen-based structures, and these are indeed consistent with the spectroscopy in the free-OH region (*31*). The unambiguous characterization of the proton environment therefore remains a challenge in this benchmark system. One complicating factor that needs to be addressed in future work is that the experimentally studied clusters are produced at finite temperatures, whereas the theoretical methods used so far do not take this into account. It may well be that dynamics resulting from the excess internal energy blurs the Eigen-Zundel structural distinction and their spectroscopic manifestations.

References and Notes

1. U. W. Schmitt, G. A. Voth, *J. Chem. Phys.* **111**, 9361 (1999).
2. D. Marx, M. E. Tuckerman, J. Hutter, M. Parrinello, *Nature* **397**, 601 (1999).
3. M. Eigen, *Angew. Chem. Int. Ed. Engl.* **3**, 1 (1964).
4. G. Zundel, in *The Hydrogen Bond — Recent Developments in Theory and Experiments. II. Structure and Spectroscopy*, P. Schuster, G. Zundel, C. Sandorfy, Eds. (North-Holland, Amsterdam, 1976), pp. 683–766.
5. N. Agmon, *Chem. Phys. Lett.* **244**, 456 (1995).
6. A. W. Castleman Jr., K. H. Bowen Jr., *J. Phys. Chem.* **100**, 12911 (1996).
7. J. Q. Searcy, J. B. Fenn, *J. Chem. Phys.* **61**, 5282 (1974).
8. J. L. Kassner Jr., D. E. Hagen, *J. Chem. Phys.* **64**, 1860 (1976).
9. S. Wei, Z. Shi, A. W. Castleman Jr., *J. Chem. Phys.* **94**, 3268 (1991).
10. R. E. Kozack, P. C. Jordan, *J. Chem. Phys.* **99**, 2978 (1993).
11. A. Khan, *Chem. Phys. Lett.* **319**, 440 (2000).
12. M. P. Hodges, D. J. Wales, *Chem. Phys. Lett.* **324**, 279 (2000).
13. M. H. Begemann, C. S. Gudeman, J. Pfaff, R. J. Saykally, *Phys. Rev. Lett.* **51**, 554 (1983).
14. K. Laasonen, M. L. Klein, *J. Phys. Chem.* **98**, 10079 (1994).
15. R. Kelterbaum, E. Kochanski, *J. Mol. Struct. (THEOCHEM)* **371**, 205 (1996).
16. M. Svanberg, J. B. C. Pettersson, *J. Phys. Chem. A* **102**, 1865 (1998).
17. J.-C. Jiang *et al.*, *J. Am. Chem. Soc.* **122**, 1398 (2000).
18. K. R. Asmis *et al.*, *Science* **299**, 1375 (2003).
19. D. W. Davidson, in *Water: A Comprehensive Treatise*, F. Franks, Ed. (Plenum, New York, 1973), vol. 2, pp. 115–234.
20. M. S. Johnson, K. T. Kuwata, C.-K. Wong, M. Okumura, *Chem. Phys. Lett.* **260**, 551 (1996).
21. M. Okumura, L. I. Yeh, J. D. Myers, Y. T. Lee, *J. Chem. Phys.* **85**, 2328 (1986).
22. M. A. Johnson, W. C. Lineberger, in *Techniques for the Study of Ion-Molecule Reactions*, J. J. M. Farrar, W. H. Saunders, Eds. (Wiley, New York, 1988), vol. 20, pp. 591.
23. M. A. Duncan, *Int. Rev. Phys. Chem.* **22**, 407 (2003).
24. At Yale, the $H^+(H_2O)_n$ clusters were prepared in an electron beam–ionized supersonic expansion, whereas the Georgia ion source uses a pulsed laser plasma on a metal target located just outside the pulsed nozzle. The electron beam ion source is also pulsed and operated under conditions close to the evaporative ensemble and likely creates ions warmer than the laser plasma source when operated in this mode. The two spectrometers differ in the time scales required for dissociation upon photoexcitation, with the Yale system allowing about 15 μs after excitation, whereas the Georgia instrument is sensitive to decay in 1 to 2 μs. Both instruments use infrared light generated by a pulsed Nd:YAG-pumped optical parametric oscillator/amplifier (LaserVision, Seattle, WA) laser. All features reported here are observed independently under all conditions. The laser plasma source (Georgia) yields similar vibrational spectra even though the intensity profile of $H^+(H_2O)_n$ clusters does not display a pronounced intensity anomaly at $n = 21$, as did the electron impact source, which yields the distribution shown in Fig. 1.
25. M. J. Frisch *et al.*, *Gaussian 03* (Gaussian, Pittsburgh, PA, 2003).
26. The calculations were performed with the Becke3LYP density functional with the aug-cc-pVDZ† basis set, which was formed by omitting the diffuse functions from the H atoms in the full aug-cc-pVDZ basis set. The geometries were optimized with the use of analytical gradients, and, for each optimized structure, the vibrational frequencies and intensities were calculated in the harmonic approximation.
27. S. McDonald, L. Ojamäe, S. J. Singer, *J. Phys. Chem. A* **102**, 2824 (1998).
28. P. J. Campagnola, L. A. Posey, M. A. Johnson, *J. Chem. Phys.* **95**, 7998 (1991).
29. C. E. Klots, *J. Chem. Phys.* **83**, 5854 (1985).
30. Z. Shi, J. V. Ford, S. Wei, A. W. Castleman Jr., *J. Chem. Phys.* **99**, 8009 (1993).
31. J.-W. Shin *et al.*, paper presented at the 227th American Chemical Society National Meeting, Anaheim, CA, 31 March 2004.

32. M.A.D., M.A.J., and K.D.J. thank NSF for support of this work under grants 0244143, 0111245, and 0078528. M.A.J. also thanks the U.S. Department of Energy under grant DE-FG02-00ER15066 for generous support of this work. K.D.J. also thanks the Pittsburgh Supercomputing Center and the Maui High Performance Computing Center for making available computational resources.

5 February 2004; accepted 5 April 2004
Published online 29 April 2004;
10.1126/science.1096466
Include this information when citing this paper.